34th Annual International Conference of the IEEE EMBS
San Diego, California USA, 28 August - 1 September, 2012

Versatile Broadband Electrode Assembly for Cell Electroporation

Yu-Hsuan Wu, Delia Arnaud-Cormos, *Member, IEEE*, Maura Casciola, Jason M. Sanders, *Student Member, IEEE*, Philippe Leveque, *Member, IEEE*, P. Thomas Vernier, *Senior Member, IEEE*

***Abstract* — In this paper, a versatile electrode assembly for cell electroporation is proposed. For validation of the delivery system, biological cell electroporation experiments using 2.5 ns and 5 ns, 10 MV/m pulsed electric fields have been conducted. Electromagnetic, time domain, and frequency analyses demonstrate the broadband behavior of the delivery system.**

I. Introduction

Electroporation can reversibly or irreversibly disrupt the integrity of the cell membrane. The electroporation phenomenon - a means for electropermeabilizing biological cell membranes under pulsed electric field - has important applications in food industries and medicine such as cancer therapy, genetic engineering, and cell biology. Classical electroporation utilizes relatively long duration (in the µs and ms range) and low voltage (a few thousand V/m) pulses [1-2]. In recent years cell membrane-related effects from pulses in the nanosecond range with amplitudes of megavolts per meter (nsPEF) have been reported [3-7]. Effects include the opening of stable and long-lasting nanopores, selective uptake of fluorescent dyes, phosphatidylserine externalization, and cell volume increase (swelling) due to water uptake. In particular, cell swelling has been recently introduced as a sensitive method for characterizing plasma membrane permeabilization [7]. However, nsPEF pulse delivery systems are challenging to construct. For an optimal energy transfer from the generator to the load, i.e. to the cells, special care must be taken to design devices compatible in terms of frequency bandwidths and impedance matching (typically 50 ohms). To increase the applied electric field and to reach the close proximity of the cells, delivery systems with reduced distances - in the micrometer range - are used. Recently, single-cell electroporation (SCEP) techniques focusing on the response at cell level have been developed [8]. Combined with automated micromanipulators [9], SCEP delivery systems provide a more flexible way to study the response of a certain cell shape, size, and orientation in the electric field. For increased flexibility in experiments involving in in-situ observations of cells after nsPEF exposure, we designed a delivery system based on tungsten wire electrodes (TWE), and we integrated it with an automated micromanipulator and a nanosecond pulse generator. We have used this system to extend our quantitative of nsPEF-induced cell swelling under a variety of conditions. The primary objectives of this paper are: describe the design and assembly of this new, versatile electrode assembly; present an electromagnetic characterization of the assemble system, particularly in terms of frequency bandwidth; validate the system with electroporation experiments with living cells.

Yu-Hsuan Wu is with the Mork Family Department of Chemical Engineering and Materials Science, VsOE, USC, Los Angeles, CA, USA.

Delia Arnaud-Cormos, Philippe Leveque are with Xlim Research Institute, UMR CNRS-University of Limoges, 123 av. A. Thomas, F-87060 Limoges, France. (corresponding author phone: +33-555-457521; fax: +33-555-457766; e-mail: delia.arnaud-cormos@xlim.fr).

Maura Casciola is with the "Sapienza" University of Rome, Italy.

Jason M. Sanders is with the Ming Hsieh Department of Electrical Engineering, VsOE, USC, Los Angeles, CA, USA.

P. Thomas Vernier is with MOSIS, Information Sciences Institute, and the Ming Hsieh Department of Electrical Engineering, Viterbi School of Engineering (VsOE), University of Southern California, Marina del Rey, CA, USA.

II. Material and Methods

Fig.1 shows the experimental set-up for nsPEF exposure of cells with the TWE. Cells placed in an 8-well coverglass chamber were exposed to 2.5 ns and 5 ns pulses from two different pulse generators, with varying pulse counts (0, 5, 10) and repetition rates (1 Hz, 1 kHz).

A. *Pulse generators*

Electrical pulses of 5 ns were applied to the TWE using a resonant-charged, solid-state Marx bank-driven, hybrid-core compression, diode-opening switch pulse generator (nsPEF1) designed and assembled at the University of Southern California (USC) [10]. Electrical pulses of 2.5 ns were applied using a laser-triggered photoconductive semiconductor switches (PCSSs) pulse generator (nsPEF2) assembled by Horus-Laser HT (Limoges, France) [11]. These generators allow to reach high electrical fields (MV/m = kV/mm) which are within or close to breakdown field strength in air. However, these fields applied for short durations in a biological solution avoid breakdown.

B. *Measurement and positioning* devices

The delivered electrical pulses were displayed on a digital storage oscilloscope (DSO, 725ZI, LeCroy, USA). A 100:1 attenuator assembled at USC was inserted in the set-up for the voltage measurement on the DSO. Three transmission lines (RG 58 C/U, Pasternack Enterprises, Irvine, USA) serve to connect the nsPEF generator to the TWE and the DSO. The applied pulses were obtained from the incident and reflected pulses using the procedure described in [12-14]. A network vector analyzer (NVA, HP 8720ET, USA) with a 20 GHz bandwidth allowed the measurement of the TWE delivery system reflection coefficient (S_{11} parameter). Observation of the cells was carried out with a Zeiss Axiovert 200 epifluorescence microscope and a Hamamatsu ImageEM CCD camera. The TWE was inserted in the 8-well coverglass chamber (Lab-Tek II, Nalge Nunc International, USA) using a 3-axis micromanipulator (MP 225/M-20139, Sutter Instruments, CA, USA) attached to the transmission line

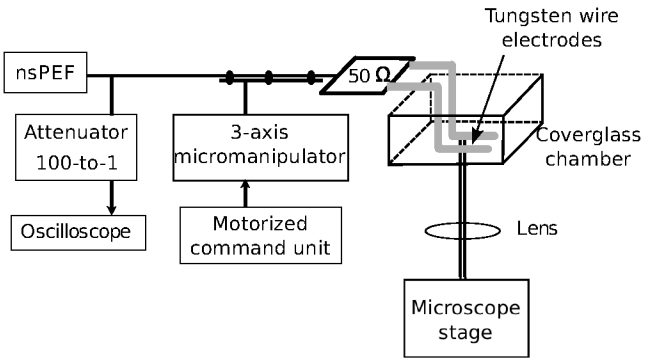

Figure 1. General experimental delivery system set-up composed of the nsPEF generator, the measurement devices, the TWE delivery system, the micromanipulator and the microscope stage.

leading to the TWE. The micromanipulator permits controlled, programmable access to the cells in the coverglass chambers on the microscope stage, quickly moving from one set of cells to another within a chamber, or from one chamber to the next.

C. *Tungsten wire electrodes*

Fig. 2 shows the assembled TWE. Two 100 µm-diameter tungsten wires were placed at a 200 µm distance, center-to-center, in a polydimethylsiloxane (PDMS) support to achieve parallel alignment. Epoxy adhesive (5 min epoxy, Pacer Technology, USA) was used to seal both ends of the channel formed by the electrodes. The gold-plated wires (45086, Alfa Aesar, MA, USA) ensure biocompatibility with the cells. To facilitate the placement of the electrodes in the coverglass well, where the cells are exposed to nsPEF, the wires were routed with a right-angle bend. The vertical part of the wires is covered with silicone rubber to give stability to the structure (Fig. 2). The wires were soldered to a BNC connector (Amphenol rfx, USA) with a 50-Ω resistor (RR5025, Vishay, PA, USA). The 50-Ω resistor placed in parallel with the TWE allows impedance matching with the transmission lines and the nsPEF generator.

D. *Cell line and imaging*

Human Jurkat T lymphoblasts (ATCC TIB-152) were grown in RPMI 1640 containing 10 % heat-inactivated fetal bovine serum, 2 mM L-glutamine, 50 units/mL penicillin, and 50 µg/mL streptomycin. Cells were cultured at 37 °C in a humidified, 5% carbon dioxide atmosphere and concentrated to 1 x 106 cells/mL for nsPEF treatment. The cells were growing using a classical culture process and placed in the Lab-Tek chamber before exposure between the electrodes. To enhance visualization of the cell outline, cells were incubated with 0.5 µM calcein-AM (acetoxymethyl ester) for 15 minutes. After incubation, cells were centrifuged and resuspended in fresh RPMI 1640 for pulse exposure. Differential interference contrast (DIC) and fluorescence images were obtained with a 63X, water-immersion objective. The images were taken as a time series, starting immediately before the pulse exposure, and at 10, 20, 30, 40, 60, 120, 180, 240 and 300 seconds after the exposure. Cell

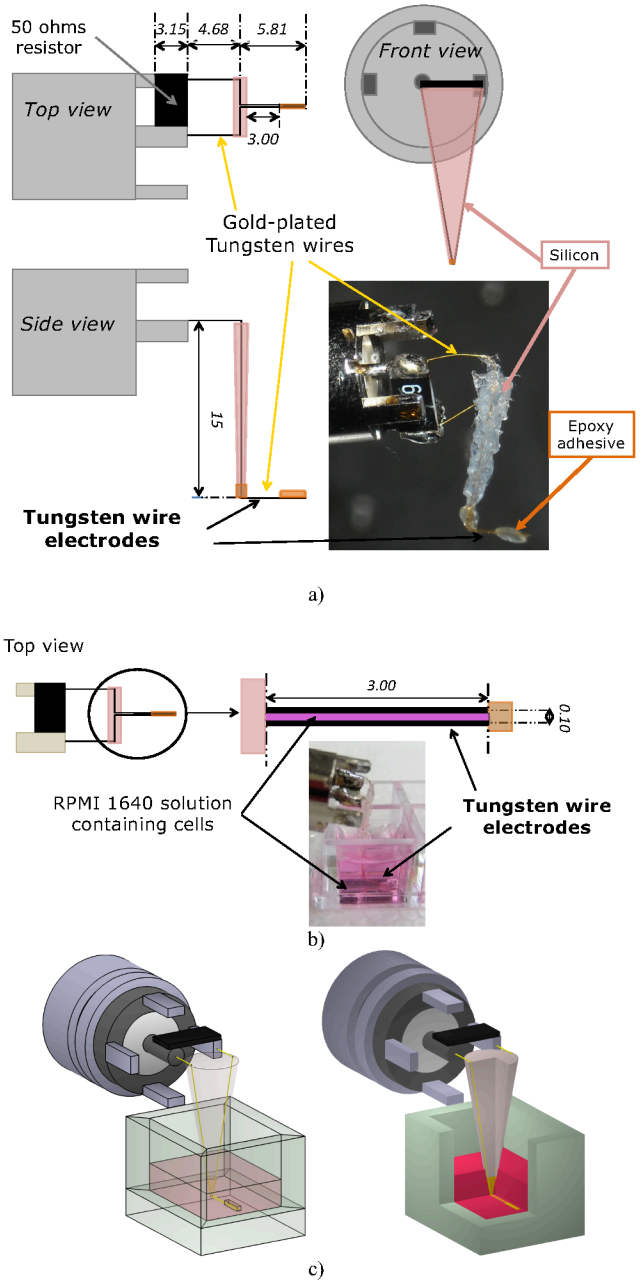

Figure 2. Tungsten wire electrode delivery system (all dimensions are in mm). a) Overview of the TWE components, materials and dimensions. b) Zoom on the TWE containing the cells under nsPEF exposure. c) View of the structure modeled with the FDTD code (left: geometry, right: meshed structure); Relative permittivity: 77 for biological medium, 6.3 for the Lab-Tek coverglass chamber, 2.1 for the BNC PTFE insulator, 3.6 for the silicone RTV and 3.7 for the epoxy adhesive.

swelling was assessed by comparing cell sizes in DIC-fluorescence merged images. Image processing was carried out with Image J 1.43u (Wayne Rasband, National Institute of Health, USA; http://rsb.info.nih.gov/ij). The cross-section of individual cells was measured, and the swelling was characterized by comparing area changes before and at different time intervals after pulse exposure.

E. FDTD numerical modeling

Electromagnetic simulations were carried out using numerical modeling of the TWE delivery system with an in-house Finite Difference-Time Domain (FDTD)-based code. Fig. 2 depicts the modeled geometry. It is composed of the BNC connector, the 50-Ω resistor, the tungsten wires vertical part covered with silicon, the TWE channel, the epoxy adhesive glue, the coverglass chamber containing the biological medium. The BNC metallic parts and the tungsten wires were considered as perfect conductors. The dielectric materials have been taken into account in the simulations through their relative permittivity (detailed on Fig. 2) and electrical conductivity (1.5 S/m for the biological medium). A non-uniform mesh was imposed in the simulations depending on the dimensions of the components. The grids used were 50×50×50 μm^3 for the TWE channel and 200×200×200 μm^3 for the other parts of the structure. The frequency behavior of the TWE delivery system through its reflection coefficient S_{11} provided by the FDTD simulations was compared to the measurements.

III. Results

A. Electromagnetic time domain and frequency analysis

To determine the generator-to-load system behavior and limitations, a time domain and frequency analysis were carried out. The measurements were performed with the TWE delivery system inserted in the coverglass chamber containing the RPMI solution and the cells, i.e corresponding to actual experimental conditions. Fig. 3 (a) shows the measured delivered (Vi) and reflected pulses (Vr is the negative pulse around 40 ns) for both generators. The reflected pulses are due to the impedance mismatch between the generator and the delivery system. The nsPEF1 delivered pulse characteristics are: 1.4-kV maximum amplitude, 5-ns FWHM (full width at half of the maximum value) and 5.0-ns rise time. The nsPEF2 delivered pulse characteristics are: 1.4-kV maximum amplitude, 2.5-ns FWHM and 1.5-ns rise time. The applied pulses, obtained by adding Vi and Vr, are plotted in Fig. 3 (b) [12-14]. Due to the attenuation introduced by the reflected pulse, the maximum amplitude of the applied pulse has decreased down to around 1.2 kV and 1.1 kV for nsPEF1 and nsPEF2, respectively. The rise times of the applied pulses have slightly increased to 6.0 ns and 1.7 ns for nsPEF1 and nsPEF2, respectively. The power spectra corresponding to the applied pulses are presented in Fig. 3 (c). The spectra are normalized with respect to the maximum value of each pulse. The -10 dB band edge, i.e the frequencies containing most of the pulses energy, is around 75 MHz and 220 MHz for nsPEF1 and nsPEF2, respectively. The -10 dB bandwidths of the applied pulses power spectra can be discussed in relation with the frequency bandwidth of the TWE delivery system. Indeed, the shorter the pulses are, the larger their frequency spectrum is, and the impedance mismatch increases with the frequency. For this purpose, the TWE delivery system reflection coefficient (S_{11}) was assessed through simulations and measurements (Fig. 4). It was measured at the input of the BNC connector (Fig. 2). Usually, the -10 dB bandwidth of $|S_{11}|$, i.e. the ratio of reflected and incident power is less than 0.1, is considered to define the limit of a good impedance matching (i.e the impedance is around 50 Ω). The results show that $|S_{11}| < -10$ dB for $f < 320$ MHz. Consequently, this TWE delivery system is adapted for delivering pulses as short as 2.5 ns. The discrepancy between FDTD simulation and measurement results above 1 GHz can be attributed to the differences between the simulated structure and the manufactured one. In addition, the value of the electric field applied between the electrodes, at the cells level i.e. at the bottom of the electrodes, of 10 MV/m was extracted from the FDTD simulations. This value is consistent with the applied voltage of 1.2 kV per 100 μm gap between circular electrodes (maximum 12 MV/m electric field can be obtained with rectangular electrodes).

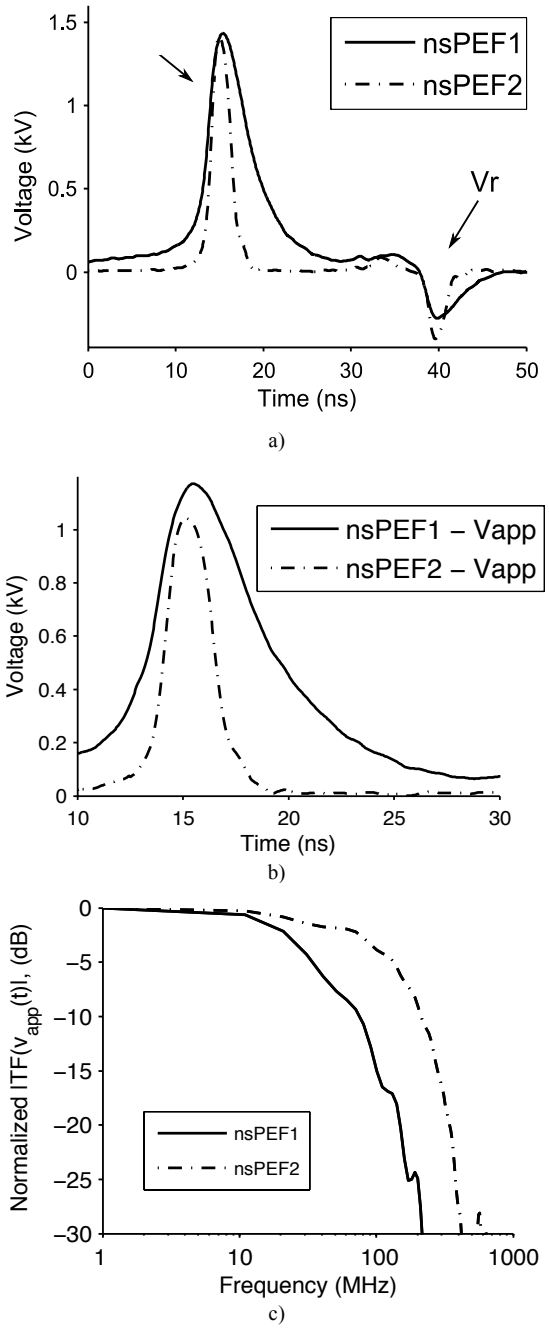

Figure 3. a) Delivered and Reflected Pulses. b) Applied Pulses. c) Normalized Power spectra in dB.

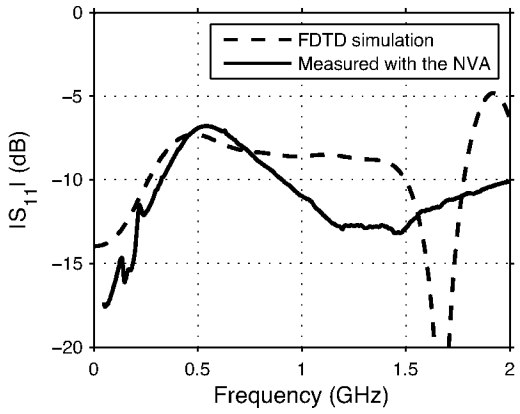

Figure 4. Frequency characterization of the TWE delivery system obtained by FDTD simulation and by measurements with a NVA. Reflection S_{11} coefficient for the TWE containing the biological medium with the cells.

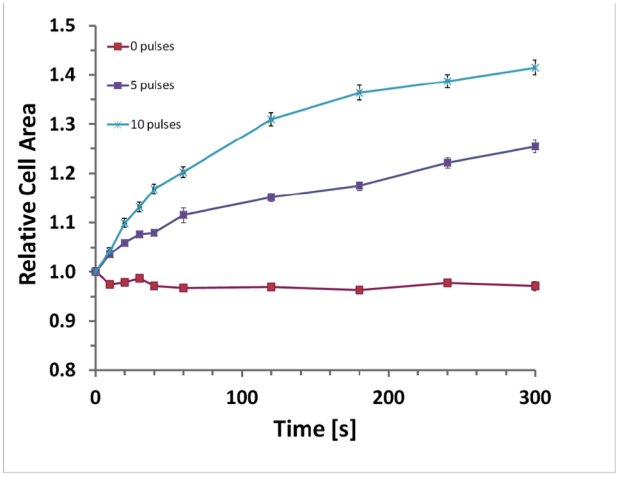

Figure 5. Dose-dependent area increase of Jurkat cells after exposure to 0, 5 and 10, 5 ns, 10 MV/m electric pulses delivered at 1 kHz. Results are presented as mean ± standard error for at least 70 cells, from at least 3 independent experiments, for each pulsing condition.

B. Biological cells exposed to 5 ns, 10 MV/m PEF

The aim of this work is to show the feasibility of the exposure apparatus. Changes in cell volume that occur as a result of membrane permeabilization-induced osmotic imbalance are used for estimating the effects of nsPEF on biological cell membrane [6]. Jurkat T lymphoblasts were exposed to 0, 5, and 10, 5.0 ns, 10 MV/m electric pulses with 1 kHz repetition rate. Fig. 5 shows that the relative cell area change is a dose-dependent effect. Under the experimental conditions, the cells were not observed to recover from swelling after 5 minutes. With these exposure parameters, the cells were reversibly electroporated.

IV. Conclusion

A versatile tungsten wire electrode assembly with dimensions suitable for real-time mammalian cell observations under nsPEF has been designed and fabricated. Electromagnetic characterization of the assembly enabled an evaluation of the actual applied pulses and fields delivered to cell suspensions. This system was used for cell electroporation with 2.5 ns and 5 ns, 10 MV/m nsPEF, and a study of cell swelling after various pulse exposures was undertaken. This broadband TWE delivery system can also be used for classical cell electroporation with µs and ms pulses.

References

[1] J. C. Weaver, "Electroporation of cells and tissues," *IEEE Trans. Plasma Sci.*, vol. 28, pp. 24-33, Feb. 2000.

[2] L. M. Mir, "Application of electroporation gene therapy: past, current, and future" *Methods Mol. Biol.*, vol. 423, pp. 3-17, 2008.

[3] P. T. Vernier, Y. Sun, and M. A. Gundersen, Nanoelectropulse-driven membrane perturbation and small molecule permeabilization, *BMC Cell Biology,* pp.7-37, 2006.

[4] A.G. Pakhomov, A.M. Bowman, B.L. Ibey, F.M. Andre, O.N. Pakhomova, K.H. Schoenbach, "Lipid nanopores can form a stable, ion channel-like conduction pathway in cell membrane," *Biochem. Biophys. Res. Commun.,* vol. 385, pp. 181–186, 2009.

[5] P.T. Vernier, M.J. Ziegler, Y. Sun, M.A. Gundersen and P. Tieleman, "Nanopore-facilitated, voltage-driven phosphatidylserine translocation in lipid bilayers—in cells and in silico," *Phys. Biol.,* vol. 3, pp. 233–247, 2006.

[6] F. M. André, M.A. Rassokhin, A.M. Bowman, A.G. Pakhomov, "Gadolinium blocks membrane permeabilization induced by nanosecond electric pulses and reduces cell death," *Bioelectrochemistry,* vol. 79, pp. 95–100, 2010.

[7] O.M. Nesin, O.N. Pakhomova, S. Xiao, A.G. Pakhomov, "Manipulation of cell volume and membrane pore comparison following single cell permeabilization with 60- and 600-ns electric pulses," *Biochimica et Biophysica Acta*, vol.1808, pp. 792–801, 2011.

[8] M. Wang, O. Orwar, J. Olofsson, and S. G. Weber, "Single-cell electroporation," *Anal Bioanal Chem,* vol. 397, pp. 3235–3248, 2010.

[9] K. Sakaki, N. Dechev, R. D. Burke, and Edward J. Park, " Development of an Autonomous Biological Cell Manipulator With Single-Cell Electroporation and Visual Servoing Capabilities," *Biomedical Engineering, IEEE Transactions on*, vol. 56, pp. 2064-2074, August 2009.

[10] Sanders, J. M., A. Kuthi, Y. H. Wu, P. T. Vernier, and M. A. Gundersen, "A linear, single-stage, nanosecond pulse generator for delivering intense electric fields to biological loads," *IEEE Trans Dielect Elect Ins,* vol. 16 pp. 1048-1054, 2009.

[11] S. El Amari, M. Kenaan, C. Merla, B. Vergne, D. Arnaud-Cormos, P. Leveque, and V. Couderc, "Kilovolt, Nanosecond, and Picosecond Electric Pulse Shaping by Using Optoelectronic Switching," *Photonics Technology Letters, IEEE,* vol. 22, pp. 1577-1579, 2010.

[12] M. Kenaan, S. El Amari, A. Silve, C. Merla, L. M. Mir, V. Couderc, D. Arnaud-Cormos, and P. Leveque, "Characterization of a 50-Ω Exposure Setup for High-Voltage Nanosecond Pulsed Electric Field Bioexperiments," Biomedical Engineering, IEEE Transactions on, vol. 58, pp. 207-214, Jan 2011.

[13] D. Arnaud-Cormos, P. Leveque, Y.-H. Wu, J. M. Sanders, M. A. Gundersen, and T. P. Vernier, "Microchamber Setup Characterization for Nanosecond Pulsed Electric Field Exposure," Biomedical Engineering, IEEE Transactions on, vol. 58, pp. 1656-1662, June 2011.

[14] S. Kohler, P. Jarrige, N. Ticaud, R. P. O'Connor, L. Duvillaret, G. Gaborit, D. Arnaud-Cormos, and P. Leveque, " Simultaneous high intensity ultrashort pulsed electric field and temperature measurements using a unique electro-optic probe," Microwave and Wireless Components Letters, IEEE, Vol. 22, pp. 153-155, March 2012.